

Supporting Information

P-doped hard carbon microspheres for sodium-ion batteries anode with superior rate and cyclic performance

Sheng Wu ^a, Handong Peng ^a, Le Huang ^a, Yongsu Liu ^a, Yanxue Wu ^b, Lei
Liu ^c, Wei Ai ^c, * and Zhipeng Sun ^{a, d}, *

^a School of Materials and Energy, Guangdong University of Technology, Guangzhou,
510006, Guangdong, China.

^b Analysis and Test Center, Guangdong University of Technology, Guangzhou,
510006, Guangdong, China.

^c Frontiers Science Center for Flexible Electronics (FSCFE) & Shaanxi Institute of
Flexible Electronics (SIFE), Northwestern Polytechnical University (NPU), 127
West Youyi Road, Xi'an 710072, China.

^d Key Laboratory of Advanced Energy Materials Chemistry (Ministry of Education),
Nankai University, Tianjin 300071, China

* Corresponding author.

E-mail address: iamwai@nwpu.edu.cn (W. Ai); zpsunxj@gdut.edu.cn (Z. Sun).

1. Experimental

1.1. Synthesis of P-doped hard carbon microspheres

In a typical synthesis process, 1.25 g poly(vinyl alcohol) (PVA, $M_w=146000-186000$) and 1.25 g sodium carboxymethyl cellulose were dissolved in 35 mL deionized water at 95 °C to form a hydrogel solution. Then 2 mL phytic acid (PA, 70% in H₂O) and 2.5 g resorcinol were dissolved in 10 mL deionized water, and the dissolved mixture was added to the above gel solution and stirred evenly. Finally, 4 mL formaldehyde (37 wt%) was added and kept stirring at 95 °C for 6 hours to obtain water-soluble phenolic resin. The gel was dried for 48 h and then heated to 800 °C (with a heating rate of 5 °C/min) for 2 h under an N₂ atmosphere. Finally, the PHCS samples were obtained, in which the amount of PA was 1, 2, and 3 mL. The PHCS samples with different amounts of PA were labeled as PHCS1 (1 mL PA), PHCS2 (2 mL PA), and PHCS3 (3 mL PA), respectively. Non-doped hard carbon microspheres (HCS) are synthesized in the same way using acetic acid.

1.2. Materials Characterizations

Microstructures of PHCS and HCS were observed by field emission scanning electron microscopy (FESEM, Hitachi SU8010, Japan) and transmission electron microscopy (TEM, Talos F200S, Czech Republic). Using high-resolution transmission electron microscopy to obtain corresponding lattice images and energy spectrum. Crystal structures and characteristics of graphitization were studied by X-Ray diffraction (XRD, D8 ADVANCE Bruker, America) with Cu K α radiation and Raman

spectroscopy (LabRAM HR Evolution, Franch) with a 532 nm laser. The electron paramagnetic resonance (EPR) measurements are carried out in a nuclear magnetic tube on a Bruker EMXPlus X-band spectrometer (Bruker EMXplus-10/12, Germany). The elemental valence and content of samples were determined by X-ray photoelectron spectroscopy (XPS, Shimadzu Axis Supra, Japan). The Brunauer-Emmett-Teller (BET) specific surface area and pore size distribution were measured by 3H-2000PS1 using the N₂ adsorption-desorption test.

1.3. Electrochemical Measurements

The working electrode was prepared by mixing the active material, superconducting carbon black, and sodium carboxymethyl cellulose according to the ratio of 8:1:1. First, add a certain amount of water to the grind to form a slurry. Then the slurry was coated on copper foil to prepare electrodes with a thickness of 100 μm. The active material on each copper foil was controlled at 0.8-1.2 mg cm⁻². Subsequently, the copper foil was dried at 60 °C for 12 hours in a vacuum, then work electrodes were cut into small pieces. The sodium metal, glass fiber diaphragm, and electrodes were assembled into a half cell in the glove box (Mikrouna) filled with Ar. All cells were worked in the electrolyte (1.0 M NaPF₆ in Diglyme). The Neware battery testing system was used to measure the galvanostatic charge/discharge curves, rate performance, and cycling performance. The cyclic voltammetry (CV) and electrochemical impedance spectroscopy (EIS) were analyzed by CHI660E electrochemical workstation. The voltage window for all electrochemical tests was 0.01-3.0 V, and the temperature was 25 °C. In order to obtain the results of *ex-situ*

analysis, all cells were discharged and charged to the corresponding potential at 0.1 A g⁻¹ in the first cycle. Then disassembled in a glove box and the electrodes are obtained by washing with 1,2 Dimethoxyethane and vacuum drying. Finally, the electrodes are transferred to an inert atmosphere container for testing.

1.4. Computational Details

All density functional theory (DFT) calculations are performed by the Vienna ab initio Simulation Package (VASP) and the projected enhanced wave method. Graphene sheets were modeled with a 6 × 6 supercell containing 72 atoms, and the geometric optimization and electronic structure were calculated using the Perdew-Burke-Ernzerhof (PBE) exchange-correlation potential within the generalized gradient approximation. Defect-carbon is simulated by deleting a C atom, and P-doped defect-carbon is simulated by replacing a C atom with a P atom. Using a cutoff energy of 400 eV, the Brillouin region integration is performed using a 2 × 2 × 1 Monkhorst-Pack k-mesh grid for structural optimization and a 4 × 4 × 1 k-mesh grid for electronic structure calculation. At the same time, all structures are kept fixed and atomic positions are completely relaxed, the convergence criteria for energy and force are set to 10⁻⁴ eV and 0.02 eV/Å, respectively. The Lz is set to be greater than 15 Å to avoid interactions between periodic images.

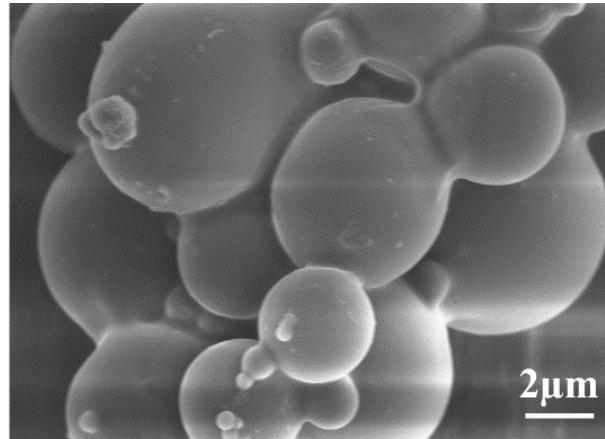


Fig. S1. The SEM images of of PHCS2 precursor

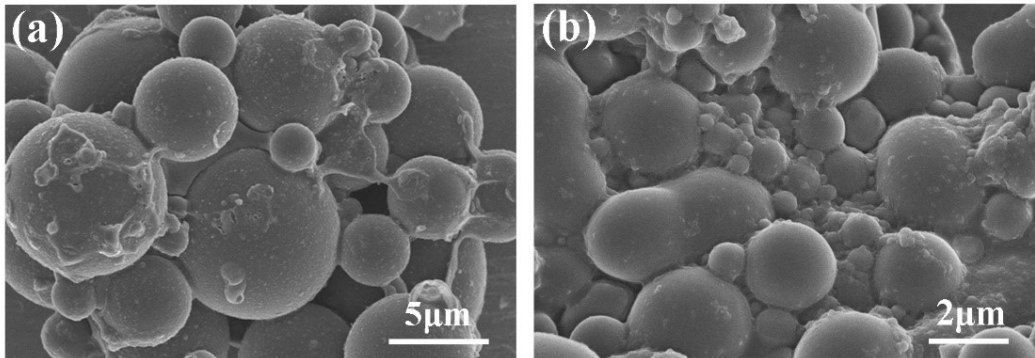


Fig. S2. (a, b) The SEM images of PHCS1 and PHCS3.

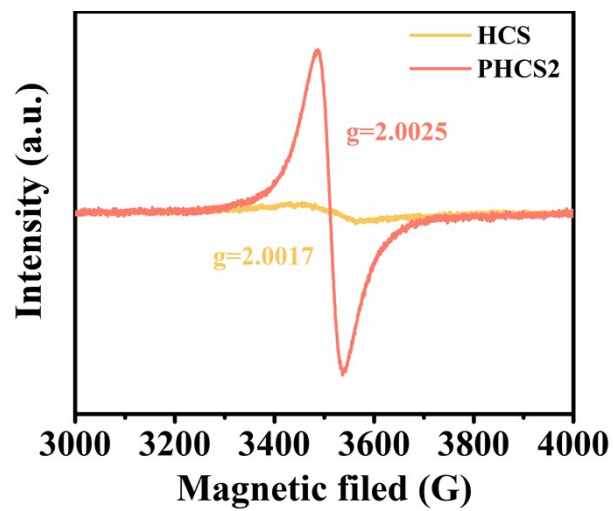


Fig. S3. EPR spectra for HCS and PHCS2.

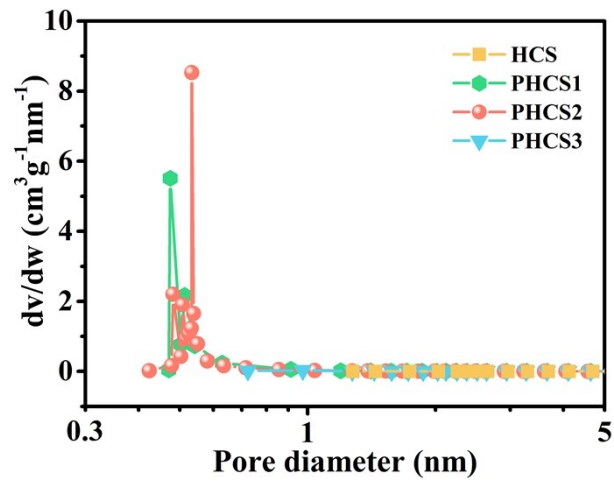


Fig. S4. Pore size distribution of PHCS and HCS.

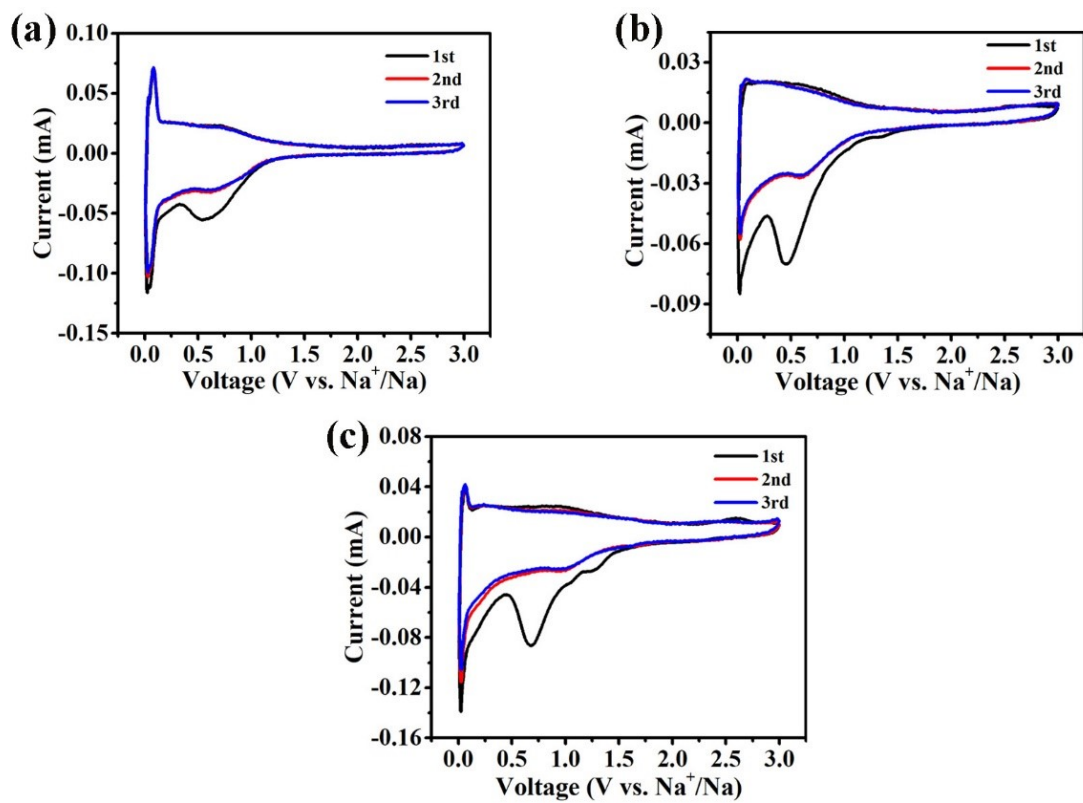


Fig. S5. (a, b, c) The cyclic voltammetry curves of HCS, PHCS1, PHCS3 at 0.1 mV s^{-1} for the first three cycles, respectively.

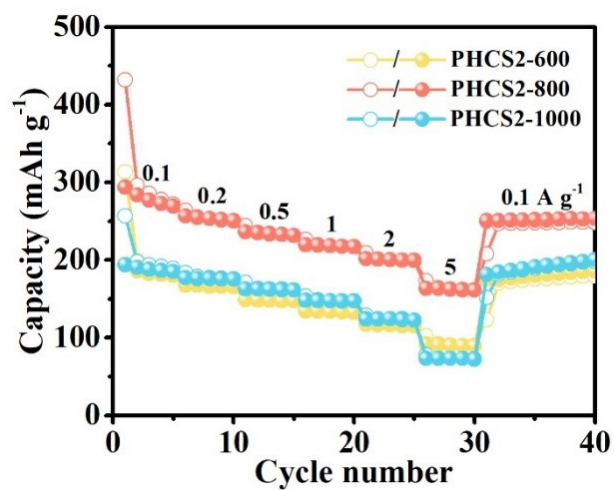


Fig. S6. Rate performance of PHCS2 at different pyrolysis temperatures.

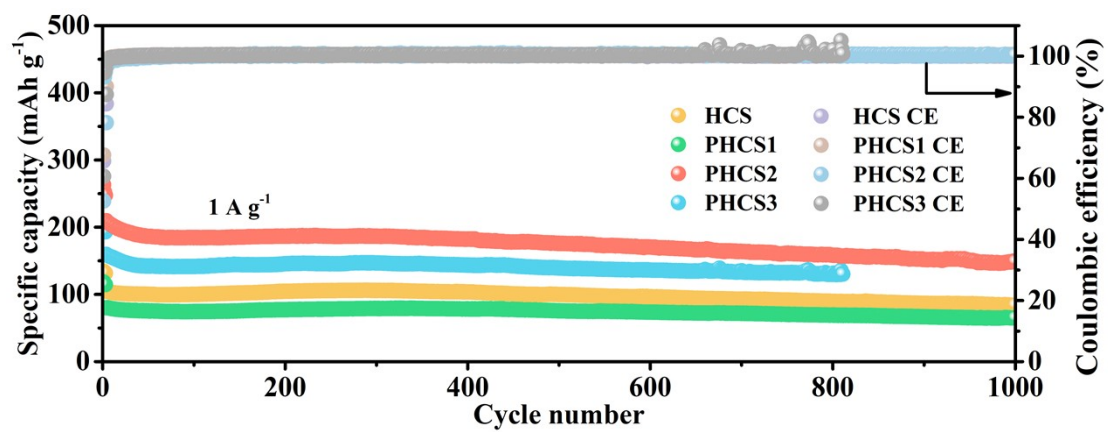


Fig. S7. Cycling performance of PHCS and HCS at 1 A g^{-1} .

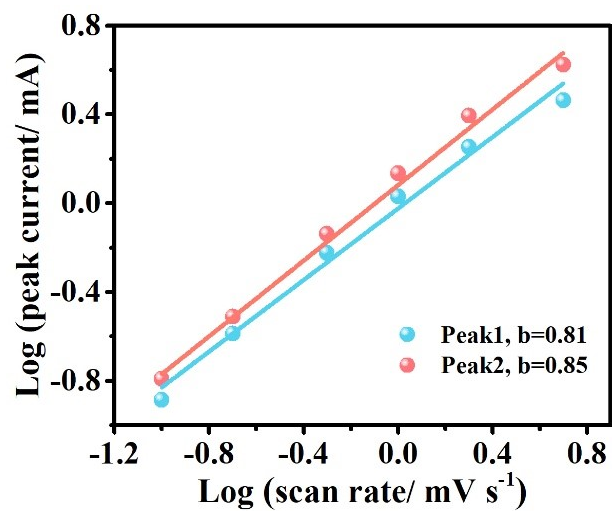


Fig. S8. Linear relationship between $\log i$ and $\log \nu$ of two peaks at 0.1-5.0 mV s⁻¹ for PHCS2.

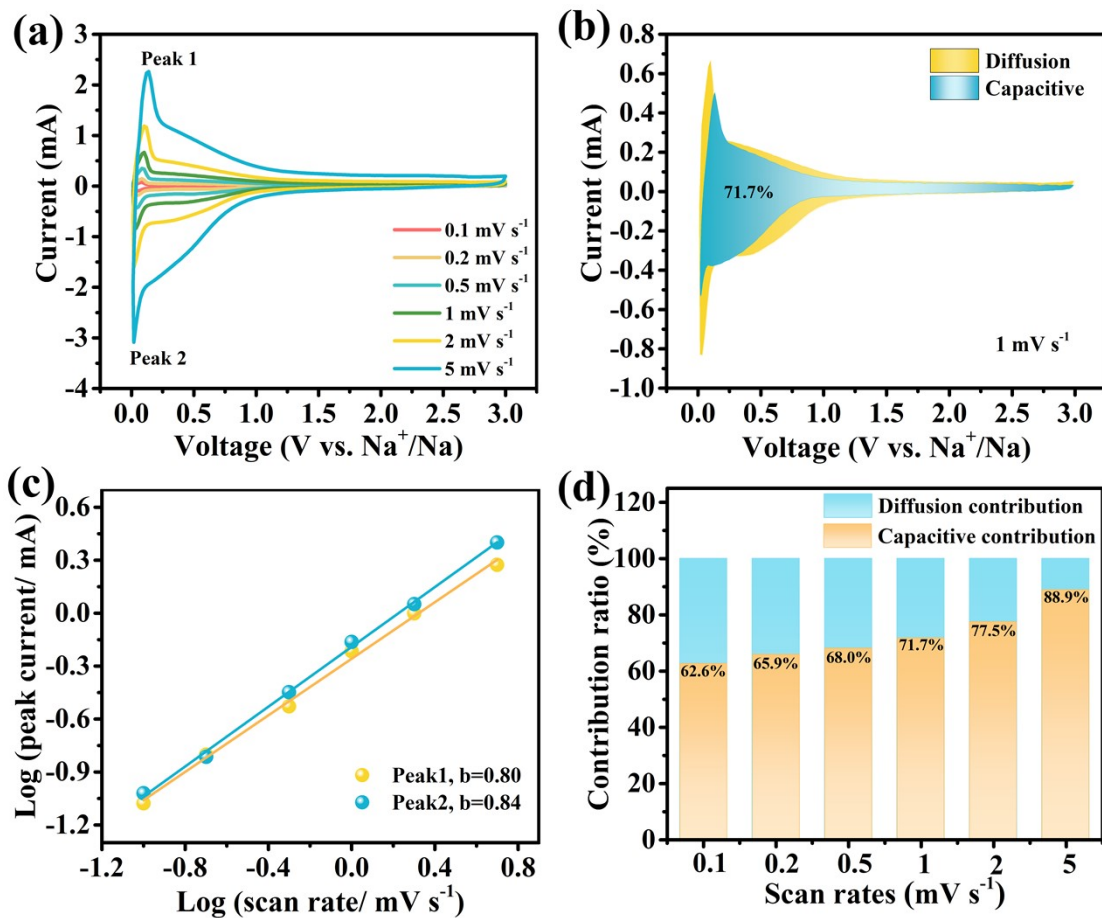


Fig. S9. Sodium ion kinetic study for HCS electrode. (a) CV graph at 0.1-5 mV s⁻¹. (b) Capacitance ratio diagram at 1 mV s⁻¹. (c) Linear relationship between log (*i*) and log (*v*) of two peaks at 0.1-5.0 mV s⁻¹. (d) Diffusion and capacitive contributions.

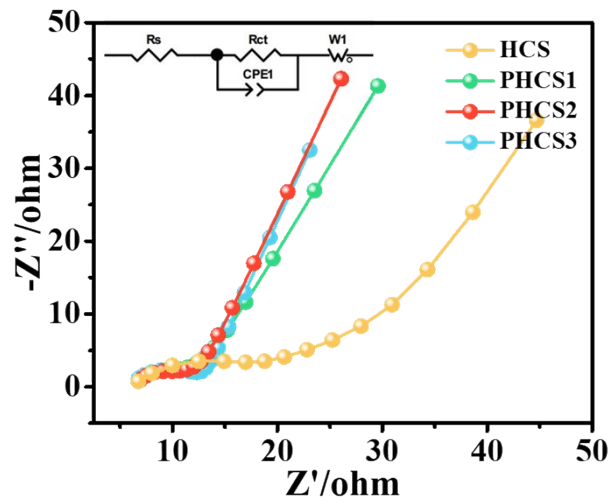


Fig. S10. The EIS plots of PHCS and HCS.

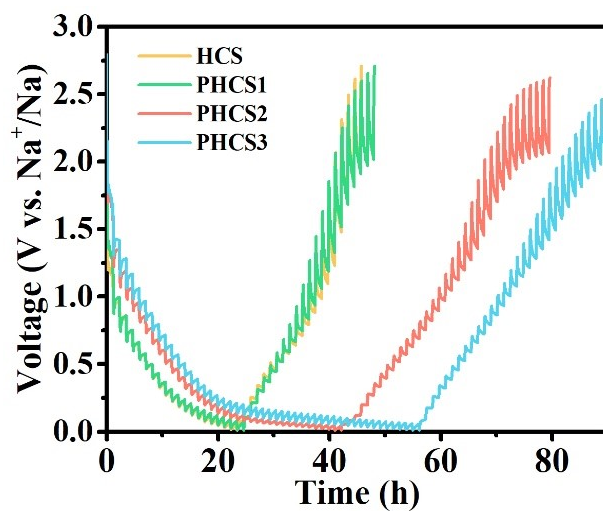


Fig. S11. Discharge and charge curves of the GITT test for PHCS and HCS.

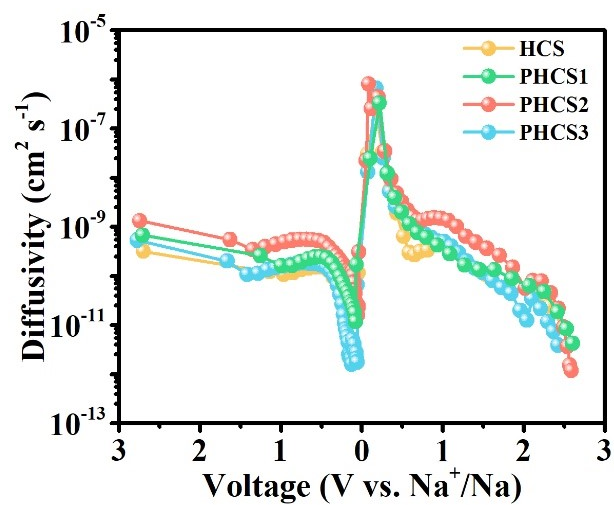


Fig. S12. The calculated diffusion coefficients of Na^+ for PHCS and HCS.

Table S1. Physical and structural parameters for all samples.

Smamples	d₀₀₂ (nm)	I_D/I_G	S_{BET} (m² g⁻¹)	V_{pore} (cm³ g⁻¹)
HCS	0.392	0.951	0.770	0.0062
PHCS1	0.394	0.957	305.051	0.1921
PHCS2	0.411	0.971	287.820	0.2160
PHCS3	0.416	0.976	46.269	0.0893

Table S2. The elemental contents tested by XPS.

Smamples	Surface composites (wt%)		
	C	O	P
HCS	84.5	15.5	0
PHCS1	86.37	11.82	1.81
PHCS2	83.15	13.86	2.99
PHCS3	81.96	13.93	4.11

Table. S3. Comparison of electrochemical performance of HCS, PHCS1, PHCS2, and PHCS3 anodes.

Smamples	ICE	Specific capacity (mAh g ⁻¹)					
		0.1 A g ⁻¹	0.2 A g ⁻¹	0.5 A g ⁻¹	1.0 A g ⁻¹	2.0 A g ⁻¹	5.0 A g ⁻¹
HCS	66.22%	131.8	117.2	105.0	95.1	84.6	66.8
PHCS1	52.10%	115.2	105.9	93.1	80.9	68.3	49.3
PHCS2	67.95%	293.5	254.8	234.8	217.4	199.7	162.5
PHCS3	58.10%	206.3	178.7	160.5	143.9	126.0	101.3

Table. S4. Comparison of electrochemical performance of PHCS2 anode with other carbon anode materials for sodium ion storage reported in previous literatures.

Material	Specific capacity	Rate Capacity		Referenc e
		Current density	Capacity	
Soft carbon nanosheets (SC-NS)	232 mAh g ⁻¹ at 0.02 A g ⁻¹	0.02 A g ⁻¹	232 mAh g ⁻¹	[17]
		1.0 A g ⁻¹	104 mAh g ⁻¹	
Hard-Soft Carbon (FP-MP 5:2 1000)	278 mAh g ⁻¹ at 0.03 A g ⁻¹	0.03 A g ⁻¹	278 mAh g ⁻¹	[19]
		1.2 A g ⁻¹	79 mAh g ⁻¹	
Hard carbon with pre-oxidation (PFHC-20)	330 mAh g ⁻¹ at 0.02 A g ⁻¹	0.02 A g ⁻¹	330 mAh g ⁻¹	[31]
		1.0 A g ⁻¹	50 mAh g ⁻¹	
Hard carbon spheres (HCS)	310 mAh g ⁻¹ at 0.05 A g ⁻¹	0.05A g ⁻¹	310 mAh g ⁻¹	[32]
		2.0 A g ⁻¹	55 mAh g ⁻¹	

Nitrogen-doped carbon sheets (NDCS)	302 mAh g ⁻¹ at 0.56 A g ⁻¹	0.56 A g ⁻¹	302 mAh g ⁻¹	[44]
		11.25 A g ⁻¹	32 mAh g ⁻¹	
N-doped HC nanoshells (N-GCNs)	325 mAh g ⁻¹ at 0.1 A g ⁻¹	0.1 A g ⁻¹	325 mAh g ⁻¹	[45]
		5.0 A g ⁻¹	63 mAh g ⁻¹	
CEM-G-8h	310 mAh g ⁻¹ at 20 mA g ⁻¹	20 mA g ⁻¹	310 mAh g ⁻¹	[46]
		0.5 A g ⁻¹	142 mAh g ⁻¹	
Ultrathin carbon nanosheets (UNCns)	270 mAh g ⁻¹ at 0.1 A g ⁻¹	0.1 A g ⁻¹	270 mAh g ⁻¹	[47]
		5.0 A g ⁻¹	139 mAh g ⁻¹	
N,O-codoped hierarchical porous hard carbon (NOHPHC)	254 mAh g ⁻¹ at 0.2 A g ⁻¹	0.2 A g ⁻¹	254 mAh g ⁻¹	[48]
		5.0 A g ⁻¹	109 mAh g ⁻¹	
N, P co-doped microspheres (NPCM)	305 mAh g ⁻¹ at 0.1 A g ⁻¹	0.1 A g ⁻¹	305 mAh g ⁻¹	[49]
		5.0 A g ⁻¹	136 mAh g ⁻¹	
PHCS2	294 mAh g ⁻¹ at 0.1 A g ⁻¹	0.1 A g ⁻¹	294 mAh g ⁻¹	This work
		5.0 A g ⁻¹	163 mAh g ⁻¹	